# Phase, timing, and amplitude noise on supercontinua generated in microstructure fiber

**Brian R. Washburn and Nathan R. Newbury**

*National Institute of Standards and Technology, 325 Broadway, Boulder, CO 80305*
brianw@boulder.nist.gov

**Abstract:** During supercontinuum formation in nonlinear fiber the presence of a noise seed on the input laser pulse can lead to significant excess noise on the generated output supercontinuum electric field. We relate pulse-averaged moments of this electric-field noise to the measured RF spectrum of the frequency comb formed by the supercontinuum. We present quantitative numerical results for the fundamental phase, timing, and amplitude noise on the frequency comb resulting from input quantum noise, including the scaling of the noise with different experimental parameters. This fundamental noise provides a lower limit to the phase stability of frequency combs that originate from microstructure fiber.

**OCIS codes:** (190.4370) Nonlinear Optics, Fibers; (120.3930) Metrological Instrumentation; (060.5530) Pulse Propagation and Solitons;

## References and Links

1. D. J. Jones, S. A. Diddams, J. K. Ranka, A. Stenz, R. S. Windeler, J. L. Hall, and S. T. Cundiff, "Carrier-envelope phase control of femtosecond mode-locked lasers and direct optical frequency synthesis," Science **288**, 635 (2000)
2. T. Udem, R. Holzwarth, and T. W. Hänsch, "Optical Frequency Metrology," Nature **416**, 233 (2002)
3. A. Baltuska, M. Uiberacker, E. Goulielmakis, R. Kienberger, V. S. Yakovlev, T. Udem, T. W. Hänsch, and F. Krausz, "Phase-controlled amplification of few-cycle laser pulses," J. Sel. Topics in Quant. Electron. **9**, 972-989 (2003)
4. L.-S. Ma, Z. Bi, A. Bartels, L. Robersson, M. Zucco, R. S. Windeler, G. Wilpers, C. Oates, L. Hollberg, and S. A. Diddams, "Optical frequency synthesis and comparison with uncertainty at the $10^{-19}$ level," Science **303**, 1843-1845 (2004)
5. J. K. Ranka, R. S. Windeler, and A. J. Stentz, "Visible continuum generation in air-silica microstructure optical fibers with anomalous dispersion at 800 nm," Opt. Lett. **25**, 25 (2000)
6. N. R. Newbury, B. R. Washburn, K. L. Corwin, and R. S. Windeler, "Noise amplification during supercontinuum generation in microstructure fiber," Opt. Lett. **28**, 944 (2002)
7. X. Gu, L. Xu, M. Kimmel, E. Zeek, P. O'Shea, A. P. Shreenath, R. Trebino, and R. S. Windeler, "Frequency-resolved optical gating and single-shot spectral measurements reveal fine structure in microstructure-fiber continuum," Opt. Lett. **27**, 1174 (2002)
8. A. L. Gaeta, "Nonlinear propagation and continuum generation in microstructured optical fibers," Opt. Lett. **27**, 924 (2002)
9. K. L. Corwin, N. R. Newbury, J. M. Dudley, S. Coen, S. A. Diddams, K. Weber, and R. S. Windeler, "Fundamental noise limitations to supercontinuum generation in microstructure fiber," Phys. Rev. Lett. **90**, 113904 (2003)
10. K. L. Corwin, N. R. Newbury, J. M. Dudley, S. Coen, S. A. Diddams, B. R. Washburn, K. Weber, and R. S. Windeler, "Fundamental amplitude noise limitations to supercontinuum spectra generated in microstructure fiber," Appl. Phys. B **77**, 269-277 (2003)
11. J. N. Ames, S. Ghosh, R. S. Windeler, A. L. Gaeta, and S. T. Cundiff, "Excess noise generation during spectral broadening in a microstructured fiber," Appl. Phys. B **77**, 279-284 (2003)
12. T. M. Fortier, J. Ye, S. T. Cundiff, and R. S. Windeler, "Nonlinear phase noise generated in air-silica microstructure fiber and its effect on carrier-envelope phase," Opt. Lett. **27**, 445-447 (2002)
13. F. W. Helbing, G. Steinmeyer, and U. Keller, "Carrier-envelope offset phase-locking with attosecond timing jitter," J. Sel. Topics in Quant. Electron. **9**, 1030-1040 (2003)
14. N. Haverkamp and H. R. Telle, "Complex intensity modulation transfer function for supercontinuum generation in microstructure fibers," Opt. Express **12**, 582-7 (2004), http://www.opticsexpress.org/abstract.cfm?URI=OPEX-12-4-582
15. J. M. Dudley and S. Coen, "Coherence properties of supercontinuum spectra generated in photonic crystal and tapered optical fibers," Opt. Lett. **27**, 1180 (2002)
16. J. W. Nicholson and M. F. Yan, "Cross-coherence measurements of supercontinua generated in highly-nonlinear, dispersion shifted fiber at 1550 nm," Opt. Express **12**, 679-688 (2004),

#4020 - $15.00 US Received 11 March 2004; revised 29 April 2004; accepted 3 May 2004

http://www.opticsexpress.org/abstract.cfm?URI=OPEX-12-4-679
17. X. Gu, M. Kimmel, A. P. Shreenath, R. Trebino, J. M. Dudley, S. Coen, and R. S. Windeler, "Experimental studies of the coherence of microstructure-fiber supercontinuum," Opt. Express **11**, 2697-2703 (2003), http://www.opticsexpress.org/abstract.cfm?URI=OPEX-11-21-2697
18. F. Lu and W. H. Knox, "Generation of broadband continuum with high spectral coherence in tapered single-mode optical fibers," Opt. Express **12**, 347-353 (2004), http://www.opticsexpress.org/abstract.cfm?URI=OPEX-12-2-347
19. D. von der Linde, "Characterization of noise in continuously operating mode-locked lasers," Appl. Phys. B **39**, 201-207 (1986)
20. H. A. Haus and A. Mecozzi, "Noise of Mode-Locked Lasers," IEEE J. Quantum Electron. **29**, 983-996 (1993)
21. J. P. Gordon and H. A. Haus, "Random walk of coherently amplified solitons in optical fiber transmission," Opt. Lett. **11**, 665-667 (1986)

## 1. Introduction

Frequency combs have proven to be powerful tools for optical frequency metrology and optical pulse synthesis [1-4]. These combs are present since the pulse train from a mode-locked laser forms a comb in frequency space with a spacing set by the repetition frequency and an offset set by the carrier-envelope offset (CEO) frequency. Stabilization of these two frequency parameters effectively stabilizes the entire comb. In order to detect the CEO frequency, the laser output is often externally spectrally broadened in microstructure fiber to generate an octave (factor of two in bandwidth) of supercontinuum [5] that can then be used in an *f*-to-2*f* interferometer [1] to generate a signal that can in turn be used to stabilize the CEO frequency. There is no fundamental reason why the 50 nm-wide tightly phase-locked comb from the passively mode-locked laser should remain a tightly phase-locked comb over the full ~500 nm of supercontinuum output. Indeed, noise on the input laser pulse can be dramatically amplified during this supercontinuum formation. Previous work has examined the excess amplitude noise on the output resulting from both technical noise [6-8] and from quantum noise [9-11] on the input laser pulse. These same noise seeds will also give rise to significant excess phase noise across the comb, which can appear as phase noise on the carrier wave, the repetition rate, or the CEO offset phase.

The conversion of input technical noise to CEO phase noise has been measured under typical conditions [12-14] and, fortunately, can be removed remarkably well through feedback. In contrast, the phase noise induced by the laser quantum noise cannot be effectively removed through feedback, and therefore represents an ultimate limit to the comb stability. The excess phase and amplitude noise is related to the optical coherence across the comb, which has been shown to be significantly degraded by input broadband noise and technical noise [15-18]. While the coherence provides a useful metric of the comb quality, this single number does not directly translate into a noise floor that will be observed in a typical heterodyne setup employing frequency combs. There are in fact four fundamental noise terms that contribute to the RF spectrum generated by heterodyning two distinct combs: amplitude jitter, phase jitter, real timing jitter, and imaginary timing jitter (i.e., frequency jitter). The CEO phase noise is a linear combination of the phase noise and timing jitter.

We first present a framework to discuss the noise in terms of the pulse-to-pulse variations in the relevant electric field moments. This framework is independent of the actual noise source. We then specifically consider the fundamental limit to the comb stability by numerically calculating the effect of the quantum vacuum fluctuations of the input pulse train on the output supercontinuum pulse train, specifically the timing noise, the phase and frequency noise on the carrier wave, the corresponding phase noise on the CEO frequency, and the amplitude noise. Our results complement and expand those of Refs. [9, 10], which examined only the amplitude noise. We discuss the basic scaling of the noise terms with optical bandwidth, input pulse quadratic phase distortion (i.e., chirp), input pulse energy, and fiber length. We find that the phase jitter, frequency jitter, and timing jitter scale similarly to the amplitude jitter; namely, the noise increases exponentially with increasing pulse energy and fiber length, and decreases exponentially as the chirp is decreased to an optimal value. As

#4020 - $15.00 US Received 11 March 2004; revised 29 April 2004; accepted 3 May 2004

a result of these strong dependencies, the noise can vary by several orders of magnitude over a reasonable range of experimental parameters. For example, the timing jitter can range from 0.01 fs to >1 fs, while the phase jitter can range from 0.3 mrad to >30 mrad. Finally, a slightly positive chirp is critical to achieving the minimum noise for a given spectral width.

## 2. Relationship between electric field noise and measured RF noise

In the basic experimental setup considered (Fig. 1), a femtosecond Ti:sapphire laser with repetition frequency $f_r \equiv T_r^{-1}$ provides a pulse train of individual, chirped, possibly noisy, hyperbolic-secant laser pulses, $E^L(t)=\Sigma_n E_n^L(t)$. After passing through the microstructure fiber, the supercontinuum is optically filtered in the spectral domain (either explicitly through a bandpass filter or implicitly through the spectral response of the receiver) to give an output comb, $E(t)=\Sigma_n E_n(t)$, where each pulse can be written as

$$E_n\left(t+nT_r\right) \approx \left(1+r_n(t)+i\vartheta_n(t)\right)E_0\left(t\right)e^{in\phi_{CEO}}, \qquad (1)$$

where $E_0(t)$ is the field of a noiseless pulse and $\phi_{CEO}$ is the CEO phase shift per pulse. The noise is described by the two real stochastic functions $r_n(t)$ and $\vartheta_n(t)$, which describe the real (in-phase) noise component and the imaginary (in-quadrature) noise component. These functions are assumed to be small (so that $\vartheta_n(t)$ also describes the phase noise), but can in principle vary dramatically across the pulse envelope. Experimentally, this electric field is not directly measured; instead a measurable RF signal is generated by mixing, or heterodyning, this field with a second electric field, which might be the comb itself, an independent second comb, a frequency doubled comb, or a narrow linewidth laser. Here, we consider two simple cases: first, a self-heterodyne signal generated by mixing the comb with itself, i.e. measuring its intensity on a photodiode; and, second, a cross-heterodyne signal generated by mixing the comb with an independent second comb with identical noise properties.

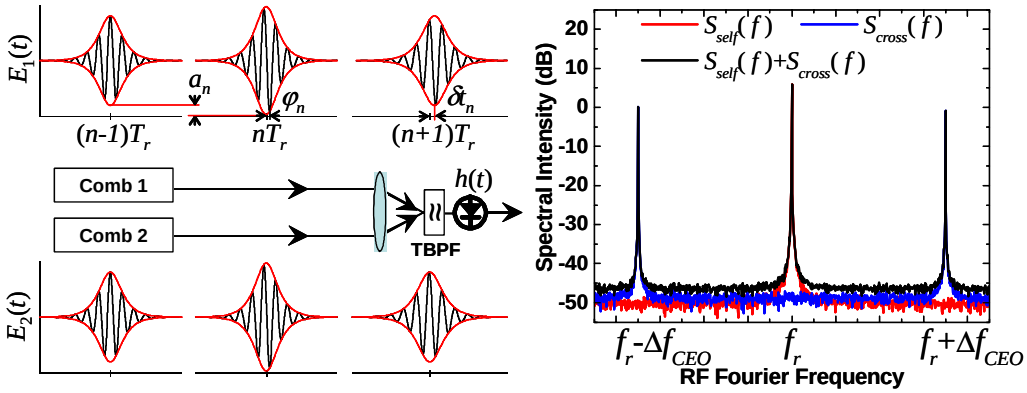


Fig. 1. Schematic showing the basic experimental setup for a heterodyne experiment. Two noisy pulse trains, exhibiting amplitude ($a_n$), phase ($\varphi_n$) and timing ($\delta t_n$) jitter, are optically filtered by a tunable bandpass filter (TBPF) and mixed on a photodetector of response $h(t)$. The resulting voltage is recorded with a RF spectrum analyzer. The contributions of the self heterodyne (red) and heterodyne (blue) parts of the total RF spectrum (black) are shown.

For a receiver with a response function $h(t)$, the received signal from a heterodyne beat between the (assumed) coincident $n^{th}$ pulses of two arbitrary comb sources (labeled ($i$) and ($j$)) is,

$$s_n\left(t\right) \approx h\left(t-t_n\right)\int E_{(i)n}\left(t'\right)E^*_{(j)n}\left(t'\right)dt' - \partial_t h\left(t-t_n\right)\int\left(t'-t_n\right)E_{(i)n}\left(t'\right)E^*_{(j)n}\left(t'\right)dt' \qquad (2)$$

plus the complex conjugate for $i \neq j$, where we have expanded the response in a Taylor series about an arrival time $t_n$. If we define the, possibly complex, arrival time as

#4020 - $15.00 US
Received 11 March 2004; revised 29 April 2004; accepted 3 May 2004

$$t_n \equiv \frac{\int t E_{(i)n}(t)\, E^*_{(j)n}(t) dt}{\int E_{(i)n}(t)\, E^*_{(j)n}(t) dt} \tag{3}$$

the second term vanishes leaving only the overlap integral.

Now, consider the simplest case of a self-heterodyne signal ($i$=$j$) in which case Eq. (2) yields the detected signal $s_{self}(t) \approx h(t) \otimes \sum_n A(1+2a_n)\delta(t - nT_r - \delta t_{R,n})$, where $\otimes$ denotes convolution and we have used Eq. (1) to describe the field. Not surprisingly, the signal depends only on the amplitude noise, which is given by the zeroth-order moment,

$$a_n \equiv A^{-1} \int r_n(t) I_0(t) dt\,, \tag{4}$$

and the timing noise, $\delta t_{R,n} = t_n - nT_r$, which, from Eq. (3), is given by first order moment,

$$\delta t_{R,n} \equiv 2A^{-1} \int r_n(t)\, t\, I_0(t) dt\,, \tag{5}$$

where the mean intensity $I_0(t) = |E_0(t)|^2$, the pulse energy $A \equiv \int I_0(t) dt$, and for convenience we define the arrival time of the unperturbed pulse as zero so that $A^{-1}\int t I_0(t) dt = 0$. The $R$ subscript on the timing noise is used to distinguish this real component of the timing noise from the imaginary component introduced later. Both these moments, Eqs. (4) and (5), are random variables with zero mean. We can describe their magnitude in frequency-space by the power spectral densities (PSDs), $S_a$ and $S_{\delta t_R}$ each defined over the Nyquist range $\pm f_r/2$. In the absence of correlations between pulses, as is the case for white noise, the PSDs are given in terms of the variances $\langle a_n^2 \rangle$ and $\langle \delta t_{R,n}^2 \rangle$ as $S_a = f_r^{-1} \langle a_n^2 \rangle$, and $S_{\delta t_R} = f_r^{-1} \langle \delta t_{R,n}^2 \rangle$ where the brackets indicate an ensemble average. The squared magnitude of the Fourier transformed signal of $s_{self}(t)$ gives the observed power spectral density for the self-heterodyne signal,

$$S_{self}(f) = |H(f)|^2 A^2 f_r^2 \left\{ \sum_n \delta(f - nf_r) + 4S_a(f - nf_r) + 4\pi^2 f^2 S_{\delta t_R}(f - nf_r) \right\}, \tag{6}$$

to first order, where $H(f)$ is the Fourier transform of the detector response function $h(t)$. Equation (6) is just a generalized version of von der Linde's classic result [19]; i.e. there is a flat amplitude noise spectrum and a quadratically increasing phase noise spectrum. The relative intensity noise (RIN) considered in Refs. [9, 10] is twice the amplitude noise term.

Now consider the second case of heterodyning a comb against another independent comb with identical noise properties and a CEO phase difference of $\Delta\phi_{CEO}$ (giving a CEO frequency difference of $\Delta f_{CEO} = f_r \Delta\phi_{CEO}/2\pi$). Using Eq. (1) to describe the electric fields, Eq. (2) then yields $s_{cross}(t) \approx h(t - nT_r) \otimes A\Sigma_n \delta(t - nT_r - \delta t_{R,n}/\sqrt{2} - \delta t_{I,n}/\sqrt{2})[1 + \sqrt{2}a_n + i\sqrt{2}\varphi_n] e^{in\Delta\phi_{CEO}}$. The signal now depends on four noise terms: the amplitude noise, the phase noise, the real timing noise, and the imaginary timing noise. The phase noise is given by the zeroth moment of $\vartheta_n(t)$,

$$\varphi_n \equiv A^{-1} \int \vartheta_n(t) I_0(t) dt\,, \tag{7}$$

in analogy to the amplitude noise, Eq. (4). The "imaginary" timing noise is given by the first moment of $\vartheta_n(t)$ (as can be derived from Eq. (3)),

$$\delta t_{I,n} \equiv 2A^{-1} \int \vartheta_n(t)\, t\, I_0(t) dt\,. \tag{8}$$

#4020 - $15.00 US Received 11 March 2004; revised 29 April 2004; accepted 3 May 2004

in analogy to Eq. (5). As discussed later this term arises from frequency jitter. Defining the PSD of the phase noise, $S_\varphi$, and the imaginary timing noise, $S_{\delta t_I}$, in analogy to their counterparts $S_a$ and $S_{\delta t_R}$, the PSD of the heterodyne, cross-product signal $s_{cross}(t)$ is

$$\begin{aligned} S_{cross}(f) = H^2(f) A^2 f_r^2 \sum\nolimits_n \delta(f - nf_r - \Delta f_{CEO}) + 2S_a(f - nf_r - \Delta f_{CEO}) \\ +2S_\varphi(f - nf_r - \Delta f_{CEO}) + 2\pi^2 f^2 S_{\delta t_R}(f - nf_r - \Delta f_{CEO}) + 2\pi^2 f^2 S_{\delta t_I}(f - nf_r - \Delta f_{CEO}), \end{aligned} \quad (9)$$

assuming no correlations between $a$ and $\delta t_I$ or $\varphi$ and $\delta t_R$. The complex conjugate of Eq. (2) gives an identical comb with the opposite sign of $\Delta f_{CEO}$. The total signal measured on an RF spectrum analyzer is the sum of these two combs and a self-heterodyne term given by Eq. (6) after quadrupling the delta-function contribution and doubling the noise terms. Figure 1 shows an example RF spectrum.

The RF spectrum, Eq. (9), is totally defined in terms of the four noise terms: the amplitude noise, Eq. (4), the phase noise, Eq. (7), the real timing noise, Eq. (5) and the imaginary timing noise, Eq. (8); only these moments affect the measured RF signal. With these definitions, we can then rewrite the noisy electric field Eq. (1) equivalently as

$$E_n(t + nT_r) \approx (1 + a_n) e^{i\varphi_n + i2\pi\delta\nu_n t} \sqrt{I_0(t - \delta t_{R,n})}\, e^{i\theta_0(t)} e^{in\phi_{CEO}}, \quad (10)$$

where the unperturbed electric field, $E_0(t) = \sqrt{I_0(t)}\, e^{i\theta_0(t)}$, has intensity $I_0(t)$ and phase $\theta_0(t)$. From Eq. (8), we can then relate the "imaginary timing jitter" directly to the carrier frequency jitter as $\delta t_{I,n} = 4\pi\delta\nu_n t^2_{RMS}$, where $t_{RMS}$ is the root-mean-square width of the pulse. These four noise terms are the same as those assumed in earlier work on the noise of mode-locked laser pulses [20]. The last noise term in Eq. (9) represents the carrier-frequency jitter "divided-down" from the inverse optical pulse width $(2\pi t_{RMS})^{-1}$ to RF frequencies. For convenience we continue to calculate the imaginary timing jitter in units of fs, rather than converting it to a frequency jitter. Figure 2 depicts the effect of the four relevant noise terms on a pulse train.

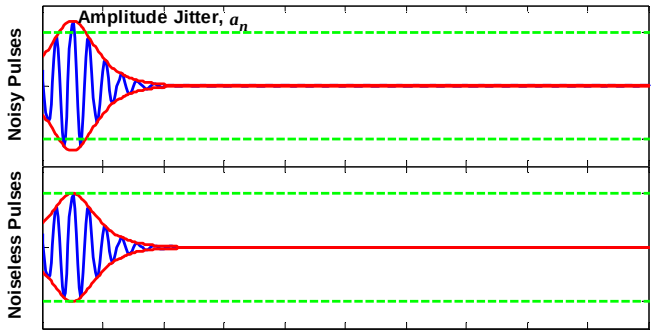


Fig. 2. (2.44 MB) A movie demonstrating the separate effect of the four jitter terms on a pulse train, compared to a noiseless pulse train. Amplitude jitter causes the peak power to vary per pulse with respect to the average. Phase jitter alters the arrival of the carrier oscillations with respect to time. The real component of the timing jitter alters the arrival time while the imaginary component is equivalent to a frequency jitter in the carrier oscillation.

None of the four moments, Eqs. (4), (5), (7), or (8) is the CEO phase. Defining the CEO phase as the intensity average of the temporal phase of the electric field pulse, $\theta_n(t)$, the noise on the CEO frequency is

$$\delta\phi_{n,CEO} \equiv \langle \theta_n(t) \rangle_n - \langle \theta_0(t) \rangle_0 \approx \varphi_n + 2\pi\nu_0 \delta t_{n,R}, \quad (11)$$

#4020 - $15.00 US
Received 11 March 2004; revised 29 April 2004; accepted 3 May 2004

where the angle brackets indicate an intensity-weighted average over the $n^{th}$ pulse and unperturbed pulse as indicated by the subscript and we have dropped terms of higher order chirp (in which case this definition is equivalent to that used in Ref. [3]). The carrier frequency $\nu_0$ is strictly given by $(2\pi)^{-1}\partial_t\theta(0)$, but since higher-order chirp is ignored we use the more convenient definition that $\nu_0$ is the intensity-averaged carrier frequency, When both carrier phase noise, $\varphi$, and timing jitter, $\delta t$, are present, the CEO phase noise depends on whether the carrier moves with or against the timing jitter (a positive $\varphi$ corresponds to the carrier moving to the "left" while a positive timing jitter corresponds to the pulse envelope moving to the "right" in Fig. 1).

The RF spectra (Eqs. (6) and (9)) assume no correlation between the four noise terms. During fiber propagation the noise terms will become correlated and additional terms should be added to account for any cross-correlations. However, as is shown later, the cross-correlation terms oscillate dramatically about zero with wavelength across the supercontinuum. Given this variation and since the RF spectrum is typically dominated by a single noise term, the cross-correlation terms are not included in the spectra for simplicity. However, over the far-infrared soliton, there is a strong extended correlation between the phase jitter, real timing jitter, and frequency jitter. The physical reason for this correlation is that this soliton moves as a packet, shifting to ever longer wavelengths as it propagates through the self-frequency shift. Thus, the envelope and underlying carrier oscillation are translated together in time.

As mentioned earlier, the noise is related to the mutual coherence of the comb, calculated in [15-18], and in our notation the modulus of the complex degree of coherence is effectively given as $1-\langle a_n^2\rangle-\langle \varphi_n^2\rangle$ for a given optical bandwidth. The coherence is a convenient single number to represent the degradation of the comb; however, it does not permit a full calculation of the noise properties since a full description of the noise require the separate calculation of the four distinct moments given in Eqs. (4), (5), (7), and (8).

### 3. Calculations for quantum input noise

The above discussion relates the noise spectra and CEO phase noise to the intensity-averaged moments of the complex multiplicative noise and is independent of the underlying noise source. In the remainder, we focus on the effects of input quantum noise. The laser pulse input to the microstructure fiber is modeled semiclassically as $E_n^L(t) = E_0^L(t) + E^{shot}(t)$ where the last noise term represents the input quantum vacuum fluctuations (responsible for shot-noise) and is delta-correlated. In Refs. [9, 10], this relatively low quantum input noise was shown to result in a noise of surprisingly large amplitude through the effects of modulation instability (MI) gain and soliton fission. These same effects will presumably result in surprisingly large phase noise as well.

To determine the output noise, we numerically solved the generalized nonlinear Schrödinger equation (NLSE) as in Refs. [6, 9, 10] assuming a microstructure fiber [5] with a nonlinearity of $\gamma$=100 $W^{-1}km^{-1}$ and the same dispersion as in Ref. [10]. For a given set of experimental parameters, such as input pulse energy, chirp, and fiber length, we generated 128 input pulses, of 45 nm spectral full width at half maximum (FWHM) centered at 810 nm, with different noise. The NLSE was used to compute the resulting supercontinuum generated by propagation of each input noisy pulse through the microstructure fiber. The resulting 128 different realizations of the supercontinuum were then processed as follows in order to generate the spectrum of the noise across the supercontinuum. First, each realization was spectrally filtered with a Gaussian filter centered at a specific wavelength. Next, the 128 different realizations of the filtered $E_n(t)$ were then used to calculate the mean field $E_0(t)$ and the jitter of the four moments given in Eqs. (4), (5), (7), and (8), which is defined as the square root of the variance. This process was then repeated for the next wavelength value across the supercontinuum (conceptually this process is equivalent to sweeping the tunable bandpass filter of Fig. 1 across the spectrum). Based on these variances and the laser repetition rate, the expected RF spectrum can be calculated directly from Eq. (6) or Eq. (9).

#4020 - $15.00 US Received 11 March 2004; revised 29 April 2004; accepted 3 May 2004

## 4. Results and discussion

Figure 3 shows the results of a typical simulation for the spectrum, phase jitter, amplitude jitter, real timing jitter, imaginary timing jitter (frequency jitter), and CEO phase jitter as a function of wavelength. As in Refs. [6, 9, 10] the noise varies dramatically with wavelength. All of the jitter terms are substantially greater than the shot noise on the output pulse. The noise terms are nevertheless small enough that the first order expansion of Eqs. (6) and (9) is valid. As mentioned previously, the cross-correlations between the noise terms oscillate strongly over the supercontinuum except across the far-infrared soliton.

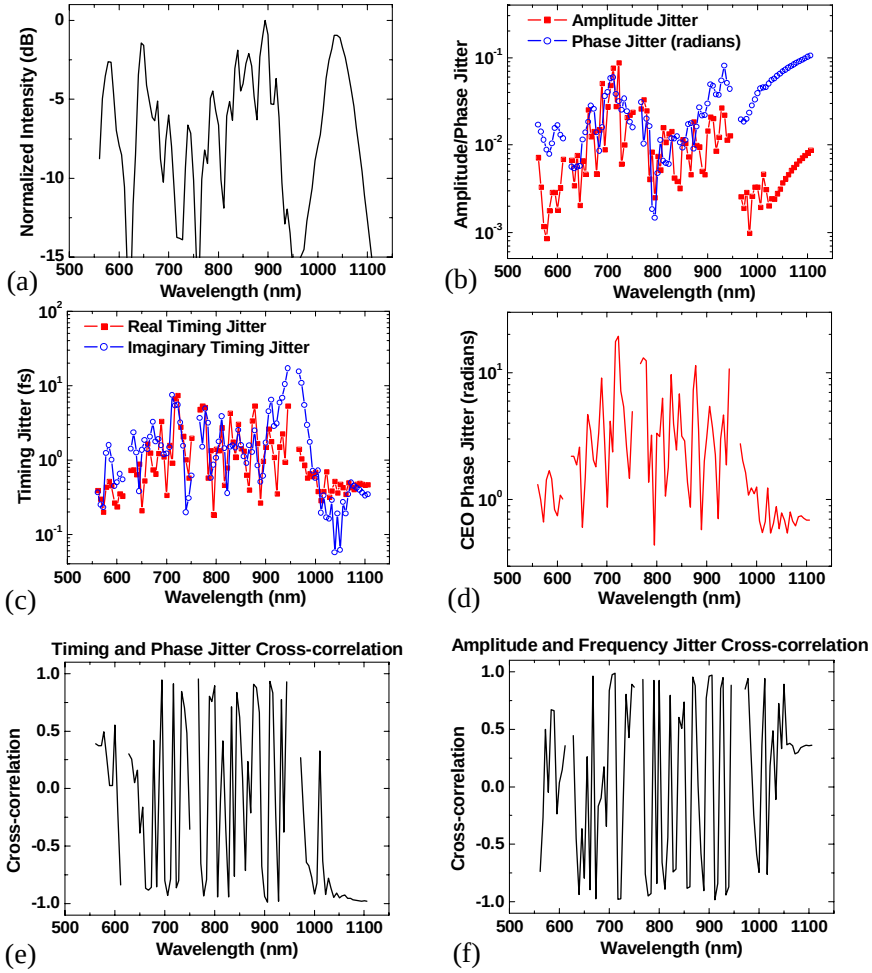


Fig. 3. (a) Supercontinuum spectrum, after filtered by a 8 nm Gaussian bandpass filter, generated by launching a 0.5 nJ laser pulse with a chirp of -282 $fs^2$ into 8 cm of fiber. (b) The amplitude and phase jitter. (c) The complex timing jitter. (d) The CEO phase jitter. (e) The cross-correlation between the real timing jitter and the phase jitter. (f) The cross correlation between the imaginary timing jitter (frequency jitter) and the amplitude jitter. The jitter, defined as the square root of the total noise variance, is not calculated for wavelengths when the filtered intensity drops below -15 dB of the peak.

#4020 - $15.00 US
Received 11 March 2004; revised 29 April 2004; accepted 3 May 2004

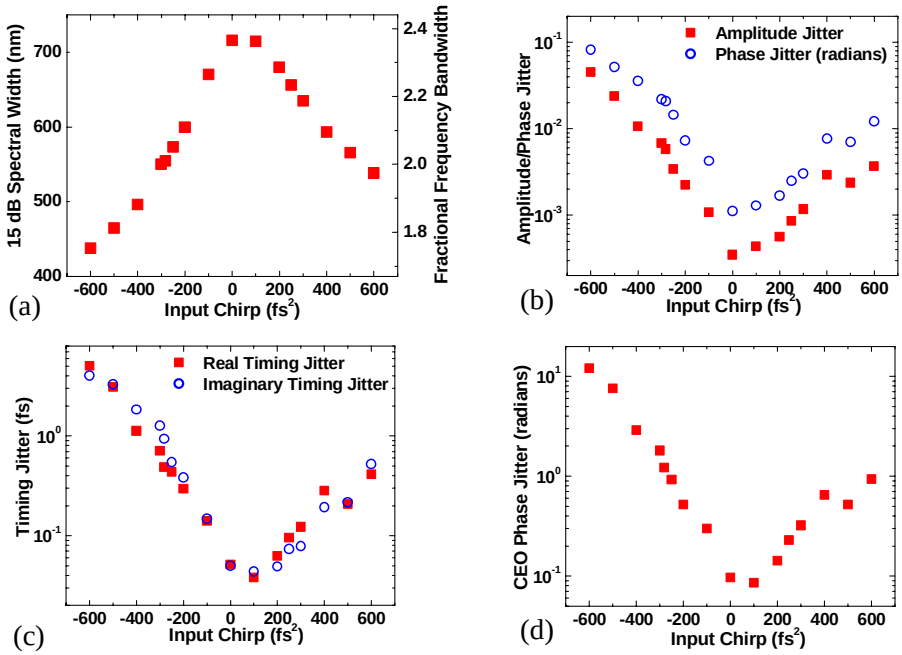


Fig. 4. (a) Median spectral width as a function of initial chirp for an input pulse energy of 0.5 nJ and a fiber length of 8 cm. (b) The median amplitude and phase jitter. (c) The median complex timing jitter. (d) The median CEO phase jitter. For an input pulse bandwidth of 45 nm, the input pulse duration changes from 15 to 90 fs as the chirp changes from 0 to ±600 fs$^2$

As described in Ref. [10], the majority of the amplitude noise generation arises from MI gain in the short length of fiber before the pulse has fissioned into individual solitons. Since the MI gain will depend exponentially on pulse power, an exponential dependence of the noise on power is also expected. More interestingly, the MI gain will also depend exponentially on the propagation length before the pulse fissions into individual solitons. Since, as shown numerically in Ref. [10], this length depends on the initial chirp value (with a minimum at a slightly positive chirp due to the combined effects of self-phase modulation and fiber dispersion), the noise will depend exponentially on chirp as well. While the discussion of Ref. [10] focused on amplitude noise, this same amplification will occur for any of the noise terms. Therefore, all the noise terms should scale similarly with the input pulse parameters. The overall magnitude of the noise terms remains undetermined from this argument, but as is discussed later there is a fairly direct connection between the magnitude of the amplitude jitter and both the phase jitter and timing jitter.

In order to capture the general behavior of the noise terms as a function of the pulse parameters, we calculate the median value across the supercontinuum spectrum. In addition, the spectral width or fractional frequency width of the supercontinuum is of interest since an octave of bandwidth (fractional frequency width of 2) is required for an *f*-to-2*f* interferometer. For all the results presented here the noise was calculated after passing the supercontinuum through a Gaussian filter with an 8 nm FWHM. The various noise terms decrease weakly with bandpass width for a range of ~2 to 20 nm. For lower widths the noise is roughly independent of the widths.

In Fig. 4, the values of spectral width and median jitter are plotted versus the input pulse quadratic phase distortion (chirp). The noise terms increase exponentially as the chirp moves from its optimal, slightly positive value. The CEO phase jitter values can be very high; however, the CEO phase on the laser pulse does not suffer from this excess noise other than any excess noise that is fed back to the laser as part of any stabilization scheme.

#4020 - $15.00 US
Received 11 March 2004; revised 29 April 2004; accepted 3 May 2004

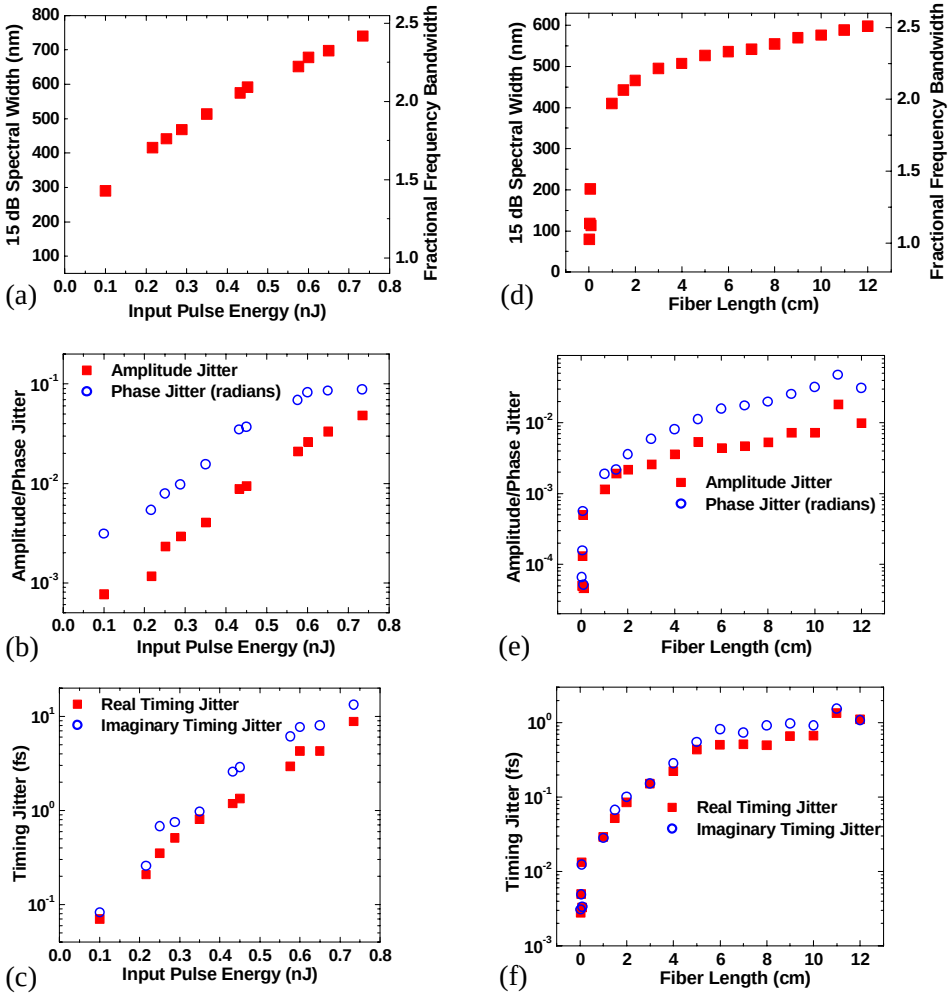


Fig. 5. (a) Median spectral width as a function of pulse energy for chirp of -282 fs$^2$ and a fiber length of 15 cm. (b) The corresponding median amplitude and timing jitter. (c) The corresponding median complex timing jitter. (d) Median spectral width as a function of fiber length for chirp of -282 fs$^2$ and an input energy of 0.5 nJ. (e) The corresponding median amplitude and timing jitter. (f) The corresponding median complex timing jitter.

In Figs. 5(a)-5(c), the same quantities are plotted as a function of pulse energy; clearly all noise quantities increase exponentially with pulse energy as expected from such a nonlinear system. In Figs. 5(d)-5(f), the same quantities are plotted as a function of fiber length. As noted in Ref. [10], most of the spectral broadening and most of the noise generation occurs in the first centimeter of the fiber. At longer lengths, there is a modest increase in spectral bandwidth with a continued buildup of the noise.

As expected, the data of Figs. 4 and 5 show that all the noise quantities scale roughly in the same manner. Since the amplitude noise is the most easily measured in a simple self-heterodyne experiment (Eq. (6)), it is interesting to relate the other terms to it. The amplitude and phase jitters are roughly equal, although the phase jitter is typically 2-3 times larger. This difference in phase and amplitude jitter is particular pronounced at longer fiber lengths and in the wings of the spectrum (see Fig. 3), where the dispersion is highest, and may be related to the Gordon-Haus effect [21]. The real and imaginary components of the timing jitter are very nearly equal. Finally, we find the timing jitter and amplitude jitter are related by $\langle \delta t_n^2 \rangle = 2\langle a_n^2 \rangle \, t_{RMS}^2$, where $t_{RMS}$ ~85 fs for the data of Fig. 4. These relationships are

#4020 - $15.00 US
Received 11 March 2004; revised 29 April 2004; accepted 3 May 2004

expected if the complex multiplicative noise of Eq. (1) is uncorrelated in time across the filtered pulse. For smaller bandwidths, the noise will grow increasingly correlated in time and this simple relationship between the amplitude noise and timing jitter begins to break down.

## 5. Conclusion

There are a number of conclusions to be drawn from the data. Perhaps the most interesting question is how the noise scales with spectral bandwidth, or, more specifically, how to achieve the largest spectral bandwidth with the minimum noise. If the spectral bandwidth is widened by 10% by increasing fiber length (beyond ~1 cm), the noise variances will increase by ~12 dB. If the spectral bandwidth is widened by 10% by increasing the input energy, the noise variances will increase by ~8 dB. On the other hand, from Fig. 4, if the spectral width is widened by 10% by decreasing the pulse chirp (toward the optimal value of +100 $fs^2$), the noise variances will *decrease* by ~12 dB. Therefore, the lowest-noise supercontinuum can be achieved with a shorter fiber and higher pulse energy and, most importantly, an initial pulse chirp set to the optimal slightly positive value. If instead the chirp is not set to the optimal value, but is allowed to vary over the possible range of 0 to ±500 $fs^2$ (corresponding to an initial pulse duration of 15 to 80 fs), and the fractional bandwidth is fixed at 2.2 by varying the input power (slightly more than the octave needed for *f*-to-2*f* detection of the CEO frequency), the timing jitter is found to range from 0.01 to 1 fs, the phase jitter from 0.3 to 30 mrad, the amplitude jitter from 0.01% to 1%, and the CEO phase jitter from 0.03 to 3 radians. The wide range of values reflects the strong dependence of the noise on chirp and input pulse energy. Given the magnitude of the different noise terms, the RF spectrum for the self-heterodyne signal, Eq. (6), is completely dominated by the amplitude noise term and is therefore flat with frequency. Similarly, the RF spectrum for the heterodyne signal from two distinct combs, Eq. (9), is completely dominated by the phase and amplitude noise terms and is also flat with frequency.

Despite the degradation in the general quality of the broad frequency comb, quantified by these various noise terms, the quality of the comb does basically remain adequate for high-precision metrology (which is unsurprising given the proven successes of the frequency comb [1-4]). For example, using the above jitter values for a chirp of +500 $fs^2$ the total noise floor for the RF spectrum detected by beating two noisy combs with 100 MHz repetition frequency has the value ~-105 dBc/Hz. This is well above the detection shot noise limit, but still yields a comfortable signal-to-noise ratio (SNR) of ~50 dB in a 300 kHz bandwidth, about 20 dB greater than needed for a good phase lock. However, this 20 dB margin cannot be taken for granted; it can rapidly disappear under the wrong experimental conditions. For example, it represents a *median* SNR over the spectrum. An unfortunate choice of wavelengths can lead to a greatly reduced SNR. Moreover, if a portion of the noise were translated through feedback to the laser cavity length into a varying time delay, $\delta t_{delay}$, between the two pulse trains, the effective phase noise of $-2\pi\nu_0\delta t_{delay}$ can easily dominate. Finally, a strong imbalance of power between the two combs, higher values of chirp, higher power levels, or fiber lengths beyond what is required to achieve an octave of bandwidth can all further dramatically reduce this 20 dB margin.

## Acknowledgments

The authors are grateful to Scott Diddams, Albrecht Bartels, Kristan Corwin, and Sarah Gilbert, and Leo Hollberg for useful discussions.

#4020 - $15.00 US Received 11 March 2004; revised 29 April 2004; accepted 3 May 2004